 CMES, vol.90, no.3, pp.211-231, 2013

Topology optimization of finite similar periodic continuum structures based on a density exponent interpolation model

Jian Hua Rong[1,2,3] **, Zhi Jun Zhao**[4] **, Yi Min Xie**[5]**, Ji Jun Yi**[1,2]

Abstract: Similar periodic structures have been widely used in engineering. In order to obtaining the optimal similar periodic structures, a topology optimization method of similar periodic structures with multiple displacement constraints is proposed in this paper. Firstly, in the proposed method, the design domain is divided into sub-domains. Secondly, a penalty term considering discrete conditions of density variables is introduced into the objective function, and the reciprocal density exponents of structural elements are taken as design variables. A topological optimization model of a similar periodic continuum structure with the objective function being the structural mass and the constraint functions being structural displacements is constructed in the proposed method. The optimization dual method is introduced and a set of iteration formula for Lagrange multipliers is built. Then, virtual sub-domain design variables are introduced to establish the relation of corresponding variables between all the sub-domains of the similar periodic continuum structure in order to enforce structurally similar periodic requirement. Three examples are provided to demonstrate that the proposed method is feasible and effective for obtaining optimal similar periodic structures.

Keywords: similar periodic structure, topological optimization, displacement constraint, quadratic programming, Lagrange multiplier

[1] School of Automotive and Mechanical Engineering, Changsha University of Science and Technology, Changsha, Hunan Province 410004, P. R. China

[2] Key Laboratory of Lightweight and Reliability Technology for Engineering Vehicle, The Education Department of Hunan Province, Changsha, 410004, China

[3] Corresponding author, Email address Rongjhua@yahoo.com.cn

[4] Department of Civil Engineering, Changsha Institute , Changsha, Hunan Province 410076, P. R. China

[5] Centre for Innovative Structures and Materials, School of Civil, Environmental and Chemical Engineering, RMIT University, GPO Box 2476, Melbourne 3001, Australia

1 Introduction

Structural topology optimization has become an effective design tool for obtaining more efficient and lighter structures. In the recent twenty years, various methods have been proposed to solve the topological optimization problem for continuum structures. Current methods of the topological optimization include the SIMP (Solid Isotropic Material with Penalty), method [Bendsøe et al., 1995, Ramm et al., 1998, Wang et al. (2008)], other optimization methods, such as the evolutionary structural optimization proposed by Xie and Steven (1993, 1997), Liang and Steven (2002), Li et al. (1999), and Rong et al. (2000, 2001, 2007), the bubble method proposed by Eschenauer and Kobelev et al. (1994), the level set method proposed by Osher and Sethian (1988, 1999), Wang et al. (2003) and Rong and Liang (2008), the ICM (Independent, Continuous and Mapping) method proposed by Sui et al. (1998, 2006), the meshless method proposed by Yuan et al. (2008), and other heuristic method proposed by Tapp et al., 2004 . The effectiveness and limitations of these optimization methods were discussed in the review papers written by Eschenauer and Olhoff (2001) and Rozvany (2009). In recent years, the topology optimization method with nodal density-based approximations [Wang et al. (2012)] and application technologies [Olyaie et al. (2011), Du et al. (2012)] have been proposed to develop the topology optimization theory and technology.

Similar periodic structures form an important branch of modern structures. These include all modular structures that are composed of certain base substructures or modules to be similarly duplicated translationally or rotationally. Typical examples are found in civil, mechanical, and aerospace engineering, such as sandwich plates, impact protecting grids, and large space trusses. Similar periodic structures have attractive advantages. The duplication of a large number of identical or similar modules significantly reduces the manufacturing cost and simplifies the assembly process. In many cases, a similar periodic geometry also exhibits a distinctive aesthetic appeal. However, a similar periodic structure generally has low efficiency in material usage due to the redundant constraint of layout periodicities. For the design of similar periodic structures, the macroscopic distribution of the designable material must be similar periodic, although the stress/strain distribution may not exhibit any similar periodic characteristics. Therefore, a general macroscopic optimization method with additional similar periodic constraints needs to be established to solve the optimization problem of a similar periodic structure efficiently.

Work on topology optimization of periodic structures can be found in the literature [Moses et al. (2003), Zhang et al. (2006), Huang et al. (2008), Zuo et al. (2011)] where the repetitive pattern is usually represented in a unit cell without the assumption of periodic boundary conditions. Since the number of unit cells is prescribed,

the size of the unit cell is determined and no scaling problem arises during the process of translating the optimization result to the manufacturing of the final product. These work [Moses et al., 2003, Zhang et al. ,2006, Huang et al., 2008, Zuo et al., 2011, Chen et al., 2010] mainly deal with the topology optimization of a periodic structure with structural natural frequency or mean compliance requirements. Recently, Xie et al. (2012) investigated the convergence of topological patterns of optimal periodic structures under multiple scales. However, the research on the topology optimization of a similar periodic structure with multiple displacement constraints is very limited at the macroscopic level under arbitrary loadings and boundaries.

This paper presents a topology optimization model of similar periodic structures with the objective function being the structural mass and the constraint functions being structural displacements by improving algorithms from the references [Rong et al. (2010,2011)]. To realize the layout similar periodicity of the optimization solution, a virtual design domain and its variables are introduced to establish a relation between any variable in the virtual design domain and a corresponding variables in all the substructures of the similar periodic continuum structure. An approximate topological optimization model for a similar periodic continuum structure is established. Then, an optimization dual method is introduced, and a set of iteration formula for solving Lagrange multipliers is built, and a set of iteration formula for topology variables for the similar periodic continuum structural optimization is established. Three examples show that the proposed method is feasible and effective for obtaining an optimal similar periodic structure.

The following sections are organized as follows. The second section is dedicated to the problem statement of the topology optimization for finite similar periodic continuum structures. The third section introduces a dual method for solving its approximate optimization problem. Before the conclusions are drawn, numerical experiments are shown with discussions.

2 Topology optimization problem of finite similar periodic continuum structures

To obtain the optimal topology of a finite similar periodic structure, the optimization design domain is divided into m sub-domains with actual sizes, as shown in Fig.1. In Fig.1, $\rho_{i,k}$ is treated as an element density variable, where i denotes the numbering of a sub-domain, and k denotes the numbering of an element in the sub-domain. For the finite periodic structure in Fig.1, the topology configuration of a sub-domain is same to the topology configuration of any other structural sub-domain along some direction (as x direction and y direction of Fig.1), namely, there are repetitive sub-structural modules in the structure. Any two sub-structural mod-

ules with a repetitive configuration may be of different sub-structural geometrical sizes for a finite similar periodic continuum structure.

Generally speaking, the number of sub-structural domains and the finite element meshes of these sub-structures are determined by engineering designers.

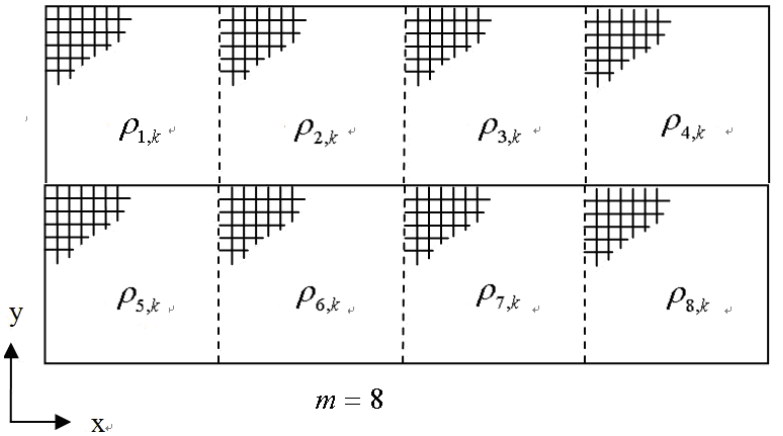

Figure 1: The optimization domain being divided into eight sub-domains

2.1 Material interpolation model

In this paper, the solid isotropic material interpolation model (1) is adopted:

$$E(\rho_{i,k}) = (\rho_{i,k})^{\alpha_k} E_0 \tag{1}$$

where $\rho_{i,k}$ is the density variable of the kth element in the ith structural sub-domain, α_k is a penalty exponent. $E(\rho_{i,k})$ is Young's modulus of the element by using material interpolation, and E_0 is the solid element Young's modulus. By referring to the reference [Rong et al. (2011)], the mass of an element can be expressed by following interpolation equation

$$w_{i,k} = (\rho_{i,k})^{\alpha_w} w_{i,k}^0 \tag{2}$$

where $w_{i,k}$ and $w_{i,k}^0$ denote the mass and the original mass of the kth element in the ith structural sub-domain, respectively. where $\alpha_w = 2$, $\alpha_k = 5$ are used in this paper.

2.2 Topology optimization model of finite similar periodic continuum structures

The topology optimization problem of similar periodic structures with multiple displacement constraints is investigated in this paper. The optimization problem of a

similar periodic structure in terms of a minimum mass approach with multiple displacement constraints, based on the density exponent interpolation model can be stated as

$$Find: \rho = \{\rho_{1,1}, \rho_{1,2}, \cdots, \rho_{1,n}, \cdots, \rho_{m,1}, \cdots, \rho_{m,n}\}^T \tag{3a}$$

$$\min \quad W \tag{3b}$$

$$s.t. \quad \left|u_j^f\right| \le U_j \quad (j = 1, \cdots, J; f = 1, 2, \cdots, L) \tag{3c}$$

$$0 < \rho_{\min} \le \rho_{i,k} \le 1 \tag{3d}$$

$$\rho_{1,k} = \rho_{2,k} = \cdots = \rho_{m,k} (i = 1, 2, \cdots, m; k = 1, 2, \cdots, n) \tag{3e}$$

where, W is the structural mass, u_j^f is the displacement of the jth degree of freedom of the structure under the fth load case, U_j is its constraint limit; L is the number of the load cases acting on the structure , and J is the number of the displacement constraints for each load case. $\rho_{\min}$ is the lower limit of element density variables. m is the number of structural sub-domains, and n is the number of elements of a structural sub-domain.

Additional constraints (3e) are listed in the optimization model so that all the sub-structures are of a same structural topology configuration.

2.3 Approximate continuous optimization model

By referring to the reference [Rong et al. (2011)] and incorporating the similar periodic requirement, a series of equivalent optimization models (4) with varied displacement constraint limits are built, in which these varied displacement constraints can limit the region of the design variable movements, and a penalty term is introduced into the objective function so that a good black/white optimal similar periodic topology can be obtained

$$Find: \rho = \{\rho_{1,1}, \rho_{1,2}, \cdots, \rho_{1,n}, \cdots, \rho_{m,1}, \cdots, \rho_{m,n}\}^T \tag{4a}$$

$$\min \quad W = \sum_{i=1}^{m} \sum_{k=1}^{n} \rho_{i,k}^{\alpha_w} w_{i,k}^0 + \gamma \sum_{i=1}^{m} \sum_{k=1}^{n} (1 - \sqrt{\rho_{i,k}^{\alpha_w}}) \sqrt{\rho_{i,k}^{\alpha_w}} w_{i,k}^0 \tag{4b}$$

$$s.t. \quad \left|u_j^f\right| \le U_j^{l\,f} \quad (j = 1, \cdots, J; f = 1, 2, \cdots, L; l = 1, 2, \cdots) \tag{4c}$$

$$0 < \rho_{\min} \le \rho_{i,k} \le 1 \tag{4d}$$

$$\rho_{1,k} = \rho_{2,k} = \cdots = \rho_{m,k}, (i = 1, 2, \cdots, m; k = 1, 2, \cdots, n) \tag{4e}$$

where U_j^{lf} is expressed as

$$U_j^{lf} = \begin{cases} \left|\bar{u}_j^f\right| + \min(\beta_1 \left|\bar{u}_j^f\right|, (\alpha_L U_j - \left|\bar{u}_j^f\right|)). & \left|\bar{u}_j^f\right| \le \alpha_L U_j \\ \left|\bar{u}_j^f\right| - \min(\beta_1 \left|\bar{u}_j^f\right|, (\left|\alpha_L U_j - \left|\bar{u}_j^f\right|\right|)). & \left|\bar{u}_j^f\right| > \alpha_L U_j \end{cases}, \quad (5)$$
$$j = 1, \cdots, J; f = 1, 2, \cdots, L$$
$$l = 1, 2, \cdots$$

where β_1 is a displacement limit changing factor, and its typical values varying between 0.04 and 0.08 are used for displacement constraints in the examples of this paper. Here, a so-called inner loop iteration process namely is a process to solve an approximate model derived from the optimization model (4), whose objective function and constraint functions are replaced by their approximate functions. Here α_L is a relaxation coefficient for the displacement constraints, and α_L=1.02 is used in the examples of this paper. $\bar{u}_j^f$ represents the displacement of the jth degree of freedom of the structure under the$f$th load case at the previous outer loop iteration step. γ is a weighted parameter for the discrete condition of all density variables $\rho_{i,k}$ $(i = 1, 2, \cdots, m; k = 1, 2, \cdots, n)$, namely $(1 - \sqrt{\rho_{i,k}^{\alpha_w}})\sqrt{\rho_{i,k}^{\alpha_w}}$=0, $(i = 1, 2, \cdots, m; k = 1, 2, \cdots, n)$. $\gamma = 0.45$ has been used in the examples in this paper.

Defining design variables $x_{i,k} = 1/(\rho_{i,k})^{\alpha_k}$ $(i = 1, 2, \cdots, m; k = 1, 2, \cdots, n)$, and incorporating the approximate expressions of the displacement constraints in the appendix, then solving Eq. (4) can be transferred to solving Eq. (6).

$$Find: x = \{x_{1,1}, x_{1,2}, \cdots, x_{1,n}, \cdots, x_{m,1}, \cdots, x_{m,n}\}^T \quad (6a)$$

$$\min: \quad \sum_{i=1}^{m}\sum_{k=1}^{n} (b_{i,k}(x_{i,k})^2 + a_{i,k}x_{i,k}) \quad (6b)$$

$$s.t. \quad \sum_{i=1}^{m}\sum_{k=1}^{n} C_{ikj}^f x_{i,k} \le D_j^f \quad (j = 1, \cdots, J;\ f = 1, 2, \cdots, L) \quad (6c)$$

$$1 \le x_{i,k} \le \bar{x}_{\max} \quad (6d)$$

$$x_{1,k} = x_{2,k} = \cdots = x_{m,k} \quad (i = 1, 2, \cdots, m; k = 1, 2, \cdots, n) \quad (6e)$$

where

$$C^f_{ikj} = ({}^j\bar{u}^{ik})^T K_0^{ik} \bar{u}^{f,ik} (\rho_{i,k}^{(l-1)})^{2\alpha_k} sign(\bar{u}^f_j) \tag{7a}$$

$$D^f_j = U^l_{j,f} - (\bar{u}^f_j - \sum_{i=1}^{m}\sum_{k=1}^{n} ({}^j\bar{u}^{ik})^T K_0^{ik} \bar{u}^{f,ik} (\rho_{i,k}^{(l-1)})^{\alpha_k}) sign(\bar{u}^f_j), _{j=1,\cdots,J,f=1,2,\cdots,L} \tag{7b}$$

$$b_{i,k} = [\frac{0.5\alpha(\alpha+1)(1-\gamma)}{\left(x_{i,k}^{(l-1)}\right)^{\alpha+2}} + \frac{0.5\alpha_1(\alpha_1+1)\gamma}{\left(x_{i,k}^{(l-1)}\right)^{\alpha_1+2}}](\frac{w^0_{i,k}}{\max\limits_{i=1,2,\cdots,m;k=1,2,\cdots,m}(w^0_{i,k})}) \tag{7c}$$

$$a_{i,k} = [\frac{-\alpha(\alpha+2)(1-\gamma)}{\left(x_{i,k}^{(l-1)}\right)^{\alpha+1}} - \frac{\alpha_1(\alpha_1+2)\gamma}{\left(x_{i,k}^{(l-1)}\right)^{\alpha_1+1}}](\frac{w^0_{i,k}}{\max\limits_{i=1,2,\cdots,m;k=1,2,\cdots,m}(w^0_{i,k})}) \tag{7d}$$

$\alpha = \alpha_w/\alpha_k$, $\alpha_1 = \alpha_w/(2\alpha_k)$, $x_{i,k}^{(l-1)} = 1/(\rho_{i,k}^{(l-1)})^{\alpha_k}$, $\bar{x}_{\max} = 1/\rho_{\min}^{\alpha_k}$.
To satisfy the positive definite condition of the objective function Hessian matrix, it is required that $b_{i,k} > 0$, which yields $\gamma < 1.75$. γ=0.45 is used in the examples of this paper.

3 Dual method for solving the approximate optimization problem

If Eq. 6e, in the optimization model is not considered, and the constant items in the objective function are omitted, solving Eq. (6) can be transferred to solving a dual optimization model (8)

$$\begin{cases} \max : \varphi(\lambda) \\ s.t. \quad \lambda \geq 0 \end{cases} \tag{8}$$

where $\phi(\lambda) = \min\limits_{1\leq x_{i,k}\leq \bar{x}_{i,k},i=1,2,\cdots,m;k=1,2,\cdots,n}(L(\mathbf{x},\lambda))$,

$$L(\mathbf{x},\lambda) = \sum_{i=1}^{m}\sum_{k=1}^{n}(b_{i,k}x_{i,k}^2 + a_{i,k}x_{i,k}) + \sum_{v=1}^{J\times L}\lambda_v(\sum_{i=1}^{m}\sum_{k=1}^{n} d_{ikv}x_{i,k} - e_v)$$

where, $d_{ik\,[(f-1)\times J+j]} = C^f_{ikj} / \max\limits_{i=1,2,\cdots,m;k=1,2,\cdots,n}(\left|C^f_{ikj}\right|)$,
$(f = 1,2,\cdots,L; j = 1,2,\cdots,J)$,

$$e_{[(f-1)*J+j]} = D^f_j / \max_{i=1,2,\cdots,m;k=1,2,\cdots,n}(\left|C^f_{ikj}\right|)$$

The one and second order partial derivatives of the objective function in the model

(8) with respect to Lagrange multipliers are derived as follows

$$\begin{aligned}\partial\phi(\lambda)/\partial\lambda_v|_{\lambda=\mathbf{0}} &= (\sum_{i=1}^{m}\sum_{k=1}^{n} d_{ikv}x_{i,k}^{*} - e_v) \\ &+ \sum_{i=1}^{m}\sum_{k=1}^{n}(2b_{i,k}x_{i,k}^{*} + a_{i,k})(\partial x_{i,k}^{*}/\partial\lambda_v)\end{aligned} \tag{9}$$

$$\begin{aligned}\partial^2\phi(\lambda)/(\partial\lambda_v\partial\lambda_r)\big|_{\lambda=\mathbf{0}} &= \sum_{i=1}^{m}\sum_{k=1}^{n} d_{ikv}\frac{\partial x_{i,k}^{*}}{\partial\lambda_r} \\ &+ \sum_{i=1}^{m}\sum_{k=1}^{n} 2b_{i,k}\frac{\partial x_{i,k}^{*}}{\partial\lambda_v}\frac{\partial x_{i,k}^{*}}{\partial\lambda_r} \\ &+ \sum_{i=1}^{m}\sum_{k=1}^{n} d_{ikr}\frac{\partial x_{i,k}^{*}}{\partial\lambda_v}\end{aligned} \tag{10}$$

The following equation may be obtained by the K-T condition and the Lagrange function.

$$\partial L(\mathbf{x},\lambda)/\partial x_{i,k} = 2b_{i,k}x_{i,k}^{*} + a_{i,k} + \sum_{v=1}^{J\times L}\lambda_v d_{ikv} = \begin{cases} \leq 0 & x_{i,k}^{*} = \bar{x}_{\max} \\ = 0 & 1 < x_{i,k}^{*} < \bar{x}_{\max} \\ \geq 0 & x_{i,k}^{*} = 1 \end{cases} \tag{11}$$

Setting $I_a = \left\{(i,k),\ 1 < x_{i,k}^{*} < \bar{x}_{\max} \quad (i = 1,2,\cdots,m; k = 1,2,\cdots,n)\right\}$ as an active design variable set, from the sensitivity of the 2th case in the equation (11) with respect to Lagrange multipliers, the Eq. (12) can be directly derived:

$$2b_{i,k}\partial x_{i,k}^{*}/\partial\lambda_v + d_{ikv} = 0 \tag{12}$$

From the equation (12), the following equations can obtained

$$\partial x_{i,k}^{*}/\partial\lambda_v = -d_{ikv}/(2b_{i,k}) \tag{13}$$

and

$$\partial^2 x_{i,k}^{*}/(\partial\lambda_v\partial\lambda_r) = 0 \tag{14}$$

Moreover, from the 1th and 3th cases in the equation (11), the following form can be obtained

$$\partial x_{i,k}^{*}/\partial\lambda_v = 0 \tag{15}$$

From Eq. (9,10) and Eq.(12-15), the one and second order partial derivatives of the objective function in the model (8) with respect to Lagrange multipliers are simplified as follows

$$\begin{aligned}\partial\phi(\lambda)/\partial\lambda_v|_{\lambda=\mathbf{0}} = &(\sum_{i=1}^{m}\sum_{k=1}^{n} d_{ikv}x^*_{i,k} - e_v) \\ &- \sum_{(i,k)\in I_a}(2b_{i,k}x^*_{i,k} + a_{i,k})d_{ikv}/(2b_{i,k})\end{aligned} \tag{16}$$

$$\partial^2\phi(\lambda)/(\partial\lambda_v\partial\lambda_r)\big|_{\lambda=\mathbf{0}} = -\sum_{(i,k)\in I_a} d_{ikv}d_{ikr}/(2b_{i,k}) \tag{17}$$

If the constant items of the second order approximation of $\varphi(\lambda)$ are omitted, the following quadratic programming model for solving Lagrange multipliers may be built.

$$\begin{cases} \min: \quad \frac{1}{2}\lambda^T D\,\lambda + H^T\lambda \\ s.t. \quad \lambda \geq 0 \end{cases} \tag{18}$$

where

$$\begin{aligned} H_v &= -\sum_{i=1}^{m}\sum_{k=1}^{n} d_{ikv}x^*_{i,k} + e_v + \sum_{(i,k)\in I_a}(2b_{i,k}x^*_{i,k} + a_{i,k})d_{ikv}/(2b_{i,k}) \\ D_{vr} &= \sum_{(i,k)\in I_a} d_{ikv}d_{ikr}/(2b_{i,k}) \end{aligned} \tag{19}$$

In this paper, $x^*_{i,k}\,(i = 1,2,\cdots,m; k = 1,2,\cdots,n)$ and λ are iteratively obtained, the design variables $x_{i,k}$ at the previous outer loop iteration step are substituted into Eq.(19) by approximately replacing $x^*_{i,k}$ in order to obtaining D and H. λ can be obtained by solving the quadratic programming model (18).

A virtual domain is constructed and introduced so that the similar periodic constraints are satisfied in the optimal topology. The topology configuration of this virtual domain is same to that of any sub-domain in the optimized structure. Setting the design variable average of kth elements in all sub-domains of the optimized structure as the design variable x_k of the kth element in this virtual domain, then the design variable x_k can be expressed as:

$$x_k = \frac{1}{m}\sum_{i=1}^{m} x_{i,k} \quad , \quad k = 1,2,\cdots,n \tag{20}$$

Considering $b_{i,k}$ $(i=1,2,\cdots,m;k=1,2,\cdots,n)$ all are positive, from Eq.(11) and Eq.(20), the following equation can be obtained

$$x_k^* + \frac{1}{m}\sum_{i=1}^{m}(a_{i,k} + \sum_{v=1}^{J\times L}\lambda_v d_{ikv})/(2b_{i,k}) \begin{cases} \leq 0 & x_k^* = \bar{x}_{\max} \\ = 0 & 1 < x_k^* < \bar{x}_{\max} \\ \geq 0 & x_k^* = 1 \end{cases} \tag{21}$$

Eq.(21) is used as an iterative formula for design variables of the virtual domain. When the design variables of the virtual domain are renewed, setting $x_{i,k} = x_k$ $(i = 1,2,\cdots,m;k=1,2,\cdots,n)$ makes that the similar periodic constraints (4e) be satisfied in the optimal topology. After obtaining $x_{i,k}(i=1,2,\cdots,m;k=1,2,\cdots,n)$, $x_{i,k}$ is treated as $x_{i,k}^*$ and is substituted into Eq.(19) to get λ by solving Eq.(18), then this new Lagrange multiplier λ is substituted into Eq.(21) , and x_k and $x_{i,k}$ are again obtained. This inner loop iteration calculation is repeated until a convergent solution is obtained. Resetting ρ^* obtained at this outer loop iteration step as ρ^l, after a new structural finite element analysis, the whole process as motioned above is repeated until the following condition is satisfied.

$$\left\|\rho^l - \rho^{(l-1)}\right\| / \left\|\rho^{(l-1)}\right\| \leq \varepsilon \tag{22}$$

To escape the checkerboard patterns of solid and void elements in the optimization process, a filtering technique proposed in the reference [Sigmund (1998)] is adopted to modify C_{ikj}^f,$a_{i,k}$and $b_{i,k}$ for all material elements. After obtaining an obvious topology configuration, this filtering technique is removed in the optimization process.

4 Examples

4.1 Beam structural topology optimization design

The first example is a beam 160 *mm* long and 40 *mm* high as shown in Fig.2a. An uniform static load of $q = 450kN/m$ is applied on the middle area along vertical directions at the most top edge of the beam as shown in Fig.2a. The thickness of the structure is 4 *mm*. The Young module E_0=200 GPa, Poisson ratio ν = 03 and mass density ρ_0 = 7800 $\mathbf{kg/m^3}$ are specified. Fig.2a shows the structural displacement boundary conditions. Fig. 2b is the finite element mesh of an initial design structure. The displacement of the point A along its vertical direction is constrained, and its displacement limit is $1.05\times10^{-4}m$ The displacement of the point B along its vertical direction is constrained, and its displacement limit also is $1.05\times10^{-4}m$. The maximum design domain is divided into a regular mesh of 240×60 with a total of 14400 equal regular four-node plane stress elements. The two layer elements located on the beam top and bottom are specified as non-design elements.

Figs.3a-3d depict optimal designs obtained by the proposed method for periodic constraints with 4×1 periodicity, 8×2 periodicity, 12×3 periodicity and 16×4 periodicity, respectively. Table 1 shows the mass and displacements at constraint points for the optimal topologies obtained by the proposed method with various periodicity requirements. From the optimization process, It can be found that the displacement constraints are satisfied, and objective functions are all convergent at the end of the optimization process. From the table 1, it can be seen that the optimal topology mass increases and the sub-domain size effect on the optimal topology mass decreases with structural periodicity increasing under the same displacement constraints. From the optimal designs obtained by the proposed method, It can be found that the design of macrostructures with periodic geometries is different from the pure material design of microstructures, and is of important engineering application value.

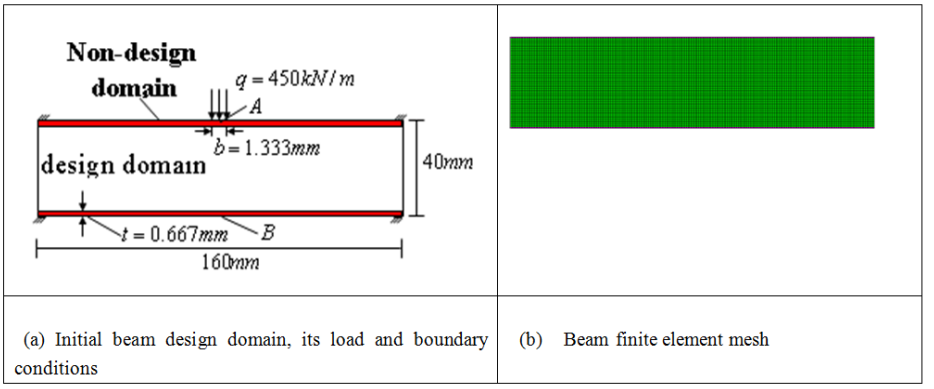

(a) Initial beam design domain, its load and boundary conditions

(b) Beam finite element mesh

Figure 2: Initial beam design domain, its load and boundary conditions, and its finite element mesh

Table 1: The masses and displacements at constraint points of the optimal topologies obtained by the proposed method with various periodicity requirements

periodicity	The total mass of the optimal topology (kg)	Displacement at point A (mm)	Displacement at point B (mm)
4×1	0.0244	0.1017	0.0149
8×2	0.0364	0.0977	0.0210
12×3	0.0409	0.1040	0.0360
16×4	0.0477	0.1029	0.0283

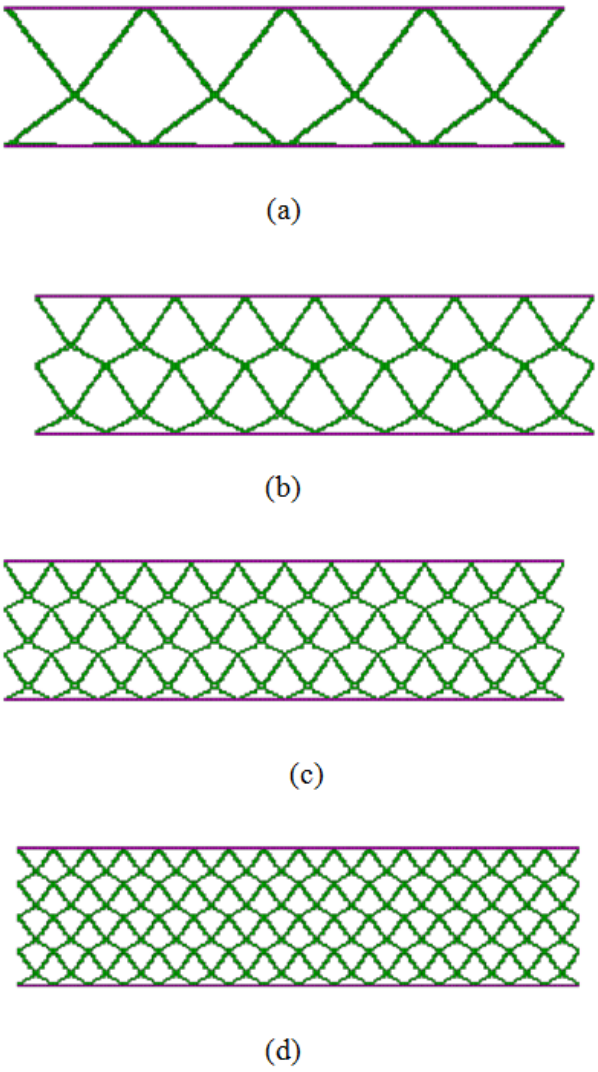

Figure 3: Optimal designs obtained by the proposed method for various periodic constraints: (a) 4×1 periodicity, (b) 8×2 periodicity; (c) 12×3 periodicity and (d) 16×4 periodicity

4.2 Topology optimization design of a roof frame

Fig.4 shows an initial structural model, its load case, displacement boundary condition and its maximum design domain of a roof frame supported by simply. In Fig.4, $L_x = 30m$, $L_{y1} = 2.1m$, $L_{y2} = 3.6m$ and $l_x = 3m$. The thickness of the structure is $0.24m$. Two load cases are specified as:$P_1 = 111kN$, $P_2 = 90kN$, $P_3 = 138kN$,$P_4 = 86kN$ and$P_5 = 169kN$ are assumed in the load case one; $P_1 = 111kN$, $P_2 = 90kN$, $P_3 = 138kN$, $P_4 = 200kN$ and $P_5 = 107kN$ are assumed in the load case two. The Young module E_0=200 GPa, Poisson ratio ν = 03 and mass density ρ_0= 7800 $\mathbf{kg/m^3}$ are specified. A displacement constraint limit at the middle point of the structural top side along its vertical direction is specified as $6mm$. Due to structural and load symmetries, only a half roof frame, as shown in Fig.5, is optimized. The maximum design domain of the half roof frame is divided into an irregular mesh of 360×50 with a total of 18000 irregular four-node plane stress elements. The two layer elements located on the roof frame top and bottom sides and the one layer elements located on the left side of the design domain are specified as non-design elements. A similar periodic topology with a similar periodicity 5×1 constraint along the horizontal direction is set.

Fig.6 shows the optimal topology of a half roof frame with 5×1 similar periodicity, obtained by the proposed method. The mass and displacement at the constraint point for the optimal topology are 30345.03kg and 5.776mm, respectively.

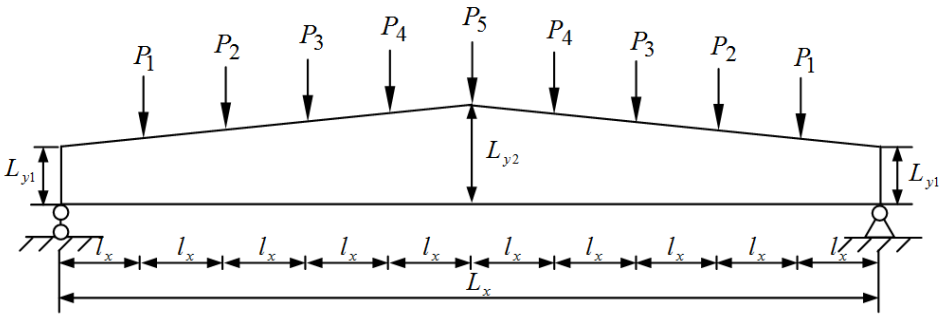

Figure 4: The initial design domain of a roof frame

4.3 Three dimensional beam topological design

Fig. 7 shows an initial structural model, its load case and its maximum design domain. An uniform static load of $\tau = 40000kN/m^2$ is applied on four areas with $0.083m \times 0.075m$ of the top plane and the bottom plane at structural left end along

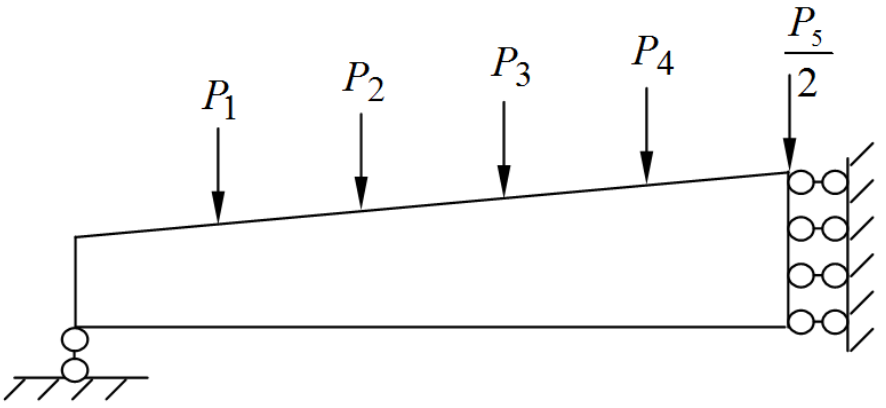

Figure 5: The initial design domain of a half roof frame

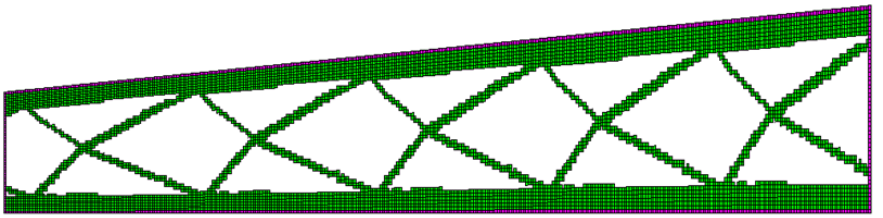

Figure 6: The optimal topology of a half roof frame with 5×1 similar periodicity, obtained by the proposed method

vertical directions. The Young module E_0=200 GPa, Poisson ratio ν = 03 and mass density ρ_0 = 7800 $\mathbf{kg/m^3}$ are specified. A displacement constraint limit at the middle point of the top side of the structural left end along vertical directions is specified as $0.0034m$, and its initial displacement is $0.193mm$. The maximum design domain of the three dimensional beam is divided into a regular mesh of $120 \times 20 \times 8$ with a total of 19200 equal regular eight-node brick elements. The two layer elements located on the beam top and bottom planes are specified as non-design elements. A periodic topology with a periodicity 4×1 constraint along the horizontal direction is specified

Fig.8 shows the optimal topology of the three dimensional beam with 4×1 periodicity, obtained by the proposed method. The mass and displacement at the constraint point for the optimal topology are $3.6114 \times 10^4 kg$ and $0.3302mm$, respectively.

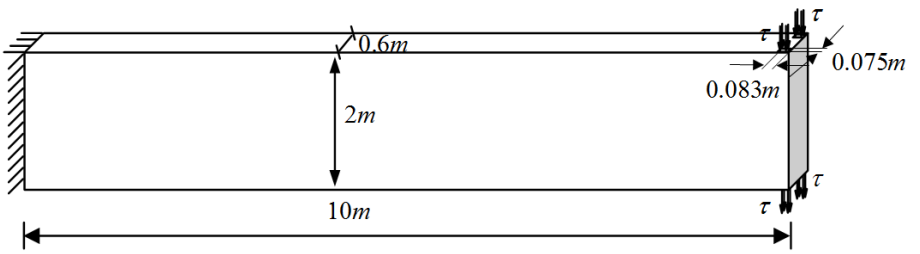

Figure 7: the initial design domain of a three dimensional beam with $4.\times1$ periodicity, its load case and displacement boundary condition

5 Conclusions

A topology optimization method of similar periodic structures with multiple displacement constraints has been developed in this paper. Additional similar periodic constraint has been added to the optimization formulation to ensure that the structure comprises a prescribed number of similar periodic substructures. The optimal similar periodic topology is obtained by an improving dual method. Several 2D and 3D examples are presented. The following conclusions can be drawn:

1) . The proposed method can be used to effectively optimize 2D and 3D similar periodic structures. The optimal design with prescribed displacement constraints, obtained by using the proposed method, will have a lower mass than the initial, guess design.

2) . The optimal topology highly depends on the total number and the aspect ratio of the similar periodic substructures.

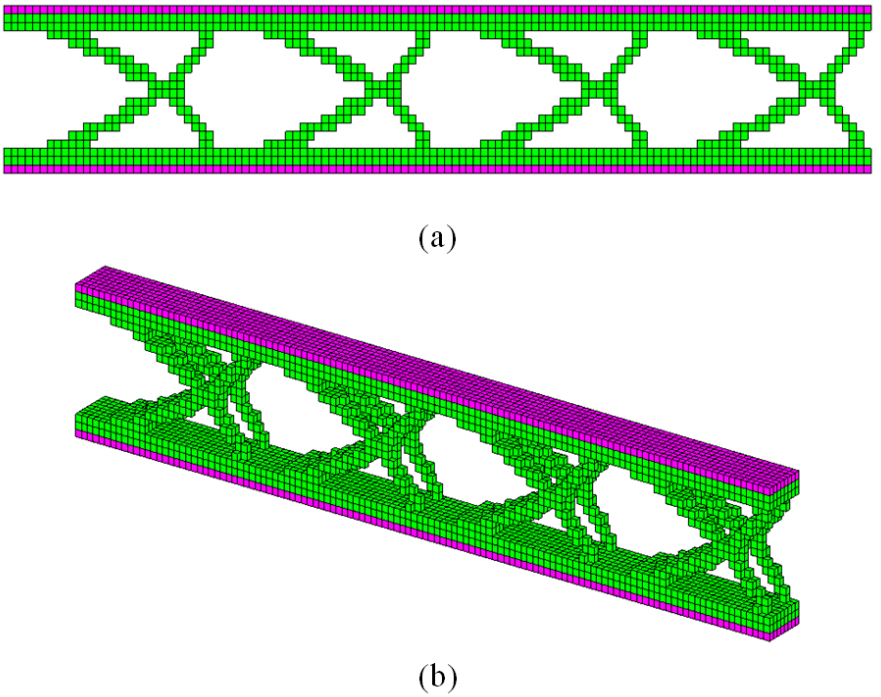

Figure 8: The optimal topology of a three dimensional beam with $4.\times 1$ periodicity obtained by the proposed method, observed from different perspectives

3) . The value of the objective function (structural mass) becomes higher when the total number of the similar periodic substructures increases. However, the advantage of a similar periodic design is that the manufacturing or construction cost could be much reduced.

Acknowledgement: This work is supported by the National Natural Science Foundation of China (10872036, 51228801), the High Technological Research and Development Program of China (2008AA04Z118).

References

Bendsøe, M.P. (1995): Optimization of Structural Topology, Shape and Material, Heidelberg, Springer.

Chen, Y.H., Zhou, S.W., Li, Q (2010): Multiobjective topology optimization for finite periodic structures. *Computers and Structures*, vol.88, pp. 806–811

Du, Y., Chen, D. (2012): Suppressing gray-scale elements in topology optimization of continua using modified optimality criterion methods. *CMES: Computer Modeling in Engineering & Sciences*, vol.86(1), pp.53-70.

Eschenauer, H.A., Kobelev, H.A., Schumacher, A. (1994), : Bubble method for topology and shape optimization of structures. *Structural Optimization*, vol.8, pp. 142–151.

Eschenauer, H.A., Olhoff, N. (2001), : Topology optimization of continuum structures: A review. *Applied Mechanics Review*, vol.54, pp. 331-390.

Huang, X., Xie, Y.M. (2008): Optimal design of periodic structures using evolutionary topology optimization. *Structural and Multidisciplinary Optimization*, vol.36, pp.597-606

Li, Q., Steven, G.P. and Xie, Y.M. (1999) , On equivalence between stress criterion and stiffness criterion in evolutionary structural optimization. *Structural and Multidisciplinary Optimization*, vol.18(1), , pp.67-73.

Liang, Q.Q. and Steven, G. P. (2002) : A performance-based optimization method for topology design of continuum structures with mean compliance constraints. *Computer Methods in Applied Mechanics and Engineering*, vol.191,1471-1489.

Moses, E., Fuchs, M.B., Ryvkin, M. (2003):Topological design of modular structures under arbitrary loading. *Structural and Multidisciplinary Optimization*, vol.24, pp.407-417.

Olyaie, M. S., Razfar, M. R., Wang, S., Kansa, E. J. (2011): Topology optimization of a linear piezoelectric micromotor using the smoothed finite element method. *CMES: Computer Modeling in Engineering & Sciences*, vol.82(1),pp. 55-82.

Osher, S. and Sethian, J.A. (1988) : Front propagating with curvature-dependent speed: Algorithms based on Hamilton–Jacobi formulations. *Journal of Computational Physics*, vol.79, pp.12–49.

Ramm, E., Maute, K., Schwarz, S. (1998): Adaptive topology and shape optimization. In: Idelshon S., Onate E. and Dvorkin E. (ed) Computational mechanics: new trends and applications. *Proceedings of the IV-world conference on computational mechanics* (CD-ROM). Barcelona, CIMNE, pp. 245-253

Rong, J.H., Jiang, J. S. and Xie, Y.M. (2007): Evolutionary structural topology optimization for continuum structures with structural size and topology variables. *Journal of Advance in Structural Engineering*, vol.10(6), pp. 681-695.

Rong, J. H. and Liang, Q.Q. (2008) : A level set method for topology optimization of continuum structures with bounded design domains. *Computer Methods in Applied Mechanics and Engineering*, vol.197(17), pp 1447-1465.

Rong, J.H., Xie, Y.M., Yang, X.Y. and Liang, Q.Q. (2000): Topology optimization of structures under dynamic response constraints. *Journal of Sound and Vibration*, vol.234 (2), pp.177-189.

Rong, J.H., Xie, Y.M. and Yang, X.Y. (2001): An improved method for evolutionary structural optimization against buckling. *Computers & Structures*, vol.79, pp. 253-263.

Rozvany, G. I. N. (2009) : A critical review of established methods of structural topology optimization. *Structural and Multidisciplinary Optimization*, vol.37, pp.217–237.

Rong, J.H., Yi, J.H. (2010): A structural topological optimization method for multi-displacement constraints and any initial topology configuration. *Acta Mechanica Sinica*, vol.26, pp.735–744.

Rong, J.H., Liu, X.H., Yi, J.J., Yi, J.H. (2011): An efficient structural topological optimization method for continuum structures with multiple displacement constraints. *Finite Elements in Analysis and Design*, vol.47, 913–921.

Sethian, J.A. (1999) , Level set methods and fast marching methods: evolving interfaces in computational geometry, fluid mechanics, computer vision, and materials Science, Cambridge University Press.

Sigmund, O, Petersson J. (1998) , Numerical instabilities in topology optimization, A survey on procedures dealing with checkerboards, mesh-dependencies and local minima. *Structural and Multidisciplinary Optimization*, vol.16, pp.68-75.

Sui, Y.K., Peng, X.R. (2006) : The ICM method with objective function transformed by variable discrete condition for continuum structure, *Acta Mechanica Sinica*, vol.22, pp.68–75.

Sui, Y.K., Yang, D.Q. (1998) , : A new method for structural topological optimization based on the concept of independent continuous variables and smooth model. *Acta Mechanica Sinica*, vol.18(2), pp.179-185.

Tapp, C., Hansel, W., Mittelstedt, C., Becker, W. (2004): Weight-minimization of sandwich structures by a heuristic topology optimization algorithm. *CMES: Computer Modeling in Engineering & Sciences*, vol. 5(6), pp. 559-573.

Wang, M.Y., Wang, X., Guo, D. (2003) : A level set method for structural topology optimization. *Computer Methods in Applied Mechanics and Engineering*, vol.192, pp.227–46.

Wang, S. Y., Lim, K. M., Khoo, B. C., Wang, M. Y. (2008): A hybrid sensitivity filtering method for topology optimization. *CMES: Computer Modeling in Engineering & Sciences*, vol.24(1), pp.21-50

Wang, Y., Luo, Z., Zhang, N. (2012): Topological optimization of structures using a multilevel nodal density-based approximation. *CMES: Computer Modeling in Engineering & Sciences*, vol.84(3), pp.229 -252

Xie, Y.M., Steven, G.P. (1993) : A simple evolutionary procedure for structural optimization, *Computers & Structures*, vol.49, pp.885–896.

Xie, Y.M., Steven, G.P. (1997), Evolutionary Structural Optimization, *Berlin: Springer-Verlag*.

Xie, Y.M., Zuo, Z.H., Huang, X., Rong, J.H. (2012), Convergence of topological patterns of optimal periodic structures under multiple scales. *Structural and Multidisciplinary Optimization*, vol.46, pp.41–50.

Yuan, W., Chen,, Y. Liu, K., Gagalowicz, A. (2008): Application of meshless local Petrov-Galerkin method in cloth simulation. *CMES: Computer Modeling in Engineering & Sciences*, vol.35(2), pp.133-156.

Zhang, W., Sun, S. (2006): Scale-related topology optimization of cellular materials and structures. *International Journal For Numerical Methods In Engineering*, vol.68, pp.993–1011.

Zuo, Z.H., Xie, Y.M., Huang, X. (2011): Optimal topological design of periodic structures for natural frequencies. *ASCE Journal of Structural Engineering*, vol.137(10), pp.1229–1240.

APPENDIX

Explicit expressions of displacement constraints

In finite element analysis, the structural static equilibrium equation under the fth load case may be expressed as

$$Ku^f = P^f \tag{A-1}$$

where K denotes the global stiffness matrix of a structure, u^f denotes the structural nodal displacement vector of the structure under the fth load case, and P^f denotes the load vector of the fth load case.

Defining $1/(\rho_{i,k})^{\alpha_k}$ as a design variable, only the stiffness matrix of the kth element in the ith structural sub-domain changes, when $1/(\rho_{i,k})^{\alpha_k}$ changes. Therefore, the partial derivative of the global stiffness matrix can be expressed as follows,

$$\partial K / \partial \left(1/(\rho_{i,k})^{\alpha_k}\right) = -\bar{K}_0^{i,k} (\rho_{i,k})^{2\alpha_k} \tag{A-2}$$

where $\bar{K}_0^{i,k}$ represents the element stiffness matrix of the kth element in the ith structural sub-domain in the global stiffness matrix dimension when the topological variable $\rho_{i,k}$ equals to unity. It is assumed that the element design variable change has no effect on the load vector P^f. We obtain the partial derivative of the displacement vector with respect to $1/(\rho_{i,k})^{\alpha_k}$ from Eq.(A1) and Eq.(A2) as

$$\partial u^f / \partial \left(1/(\rho_{i,k})^{\alpha_k}\right) = (\rho_{i,k})^{2\alpha_k} K^{-1} \bar{K}_0^{i,k} u^f \tag{A-3}$$

To find the partial derivative of u_j^f with respect to $1/(\rho_{i,k})^{\alpha_k}$, an unit virtual load vector F^j is introduced, in which only the jth component is equal to unity and all the others are equal to zero. Multiplying both sides of Eq. (A3) by $(F^j)^T$, following equation can be obtained

$$\begin{aligned} \partial u_j^f / \partial \left(1/(\rho_{i,k})^{\alpha_k}\right) &= (\rho_{i,k})^{2\alpha_k} (F^j)^T K^{-1} \bar{K}_0^{i,k} u^f \\ &= (\rho_{i,k})^{2\alpha_k} ({}^j u)^T \bar{K}_0^{i,k} u^f \\ &= (\rho_i)^{2\alpha_k} ({}^j u^{i\,k})^T K_0^{i,k} u^{f,\,i\,k} \end{aligned} \tag{A-4}$$

where ${}^j u$ is the displacement due to the unit load F^j, $K_0^{i,k}$ is the element stiffness matrix of the kth element in the ith structural sub-domain when the topological variable $\rho_{i,k}$ equals to unity. $u^{f,\,i\,k}$ and ${}^j u^{i\,k}$ are the element displacement vectors containing the entries of u^f and ${}^j u$ respectively, which are related to the kth element in the ith structural sub-domain. The computation of the right hand side of equation (A4) can be done at element level.

Therefore, the one order approximation of u_j^f at the design point $x_{i,k}^{(l-1)} = 1/(\rho_{i,k}^{(l-1)})^{\alpha_k}$ $(i = 1,2,\cdots,m; k = 1,2,\cdots,n)$, where $x_{i,k}^{(l-1)}$ denotes the design variables obtained

at the $(l-1)$th outer loop iteration step , can be expressed as,

$$\begin{aligned} u_j^f &= \bar{u}_j^f + \sum_{i=1}^{m}\sum_{k=1}^{n} (u_j^f)'_{x_{i,k}}\Big|_{x^{(l-1)}} (x_{i,k} - x_{i,k}^{(l-1)}) \\ &= \bar{u}_j^f + \sum_{i=1}^{m}\sum_{k=1}^{n} ({}^j\bar{u}^{ik})^T K_0^{ik} \bar{u}^{f,ik} \frac{1}{(x_{i,k}^{(l-1)})^2} (x_{i,k} - x_{i,k}^{(l-1)}) \\ &= \left(\bar{u}_j^f - \sum_{i=1}^{m}\sum_{k=1}^{n} ({}^j\bar{u}^{ik})^T K_0^{ik} \bar{u}^{f,ik} (\rho_{i,k}^{(l-1)})^{\alpha_k} \right) \\ &+ \sum_{i=1}^{m}\sum_{k=1}^{n} ({}^j\bar{u}^{ik})^T K_0^{ik} \bar{u}^{f,ik} \frac{(\rho_{i,k}^{(l-1)})^{2\alpha_k}}{(\rho_{i,k})^{\alpha_k}} \end{aligned} \tag{A-5}$$

where $\bar{u}_j^f$, ${}^j\bar{u}^{ik}$and $\bar{u}^{f,ik}$ are u_j^f, ${}^j u^{ik}$ and $u^{f,i}$ at the , $(l-1)$th outer loop iteration step, respectively.